Identification of Critical Transmission Limits in Injection Impedance Plane

Jóhannsson, Hjörtur; Østergaard, Jacob; Nielsen, Arne Hejde

Published in:
International Journal of Electrical Power & Energy Systems

Link to article, DOI:
10.1016/j.ijepes.2012.05.050

Publication date:
2012

Document Version
Publisher's PDF, also known as Version of record

AUTHOR QUERY FORM

ELSEVIER	**Journal: JEPE** **Article Number: 1805**	**Please e-mail or fax your responses and any corrections to:** **E-mail: corrections.esch@elsevier.sps.co.in** **Fax: +31 2048 52799**

Dear Author,

Please check your proof carefully and mark all corrections at the appropriate place in the proof (e.g., by using on-screen annotation in the PDF file) or compile them in a separate list. Note: if you opt to annotate the file with software other than Adobe Reader then please also highlight the appropriate place in the PDF file. To ensure fast publication of your paper please return your corrections within 48 hours.

For correction or revision of any artwork, please consult http://www.elsevier.com/artworkinstructions.

Any queries or remarks that have arisen during the processing of your manuscript are listed below and highlighted by flags in the proof. Click on the 'Q' link to go to the location in the proof.

Location in article	Query / Remark: click on the Q link to go Please insert your reply or correction at the corresponding line in the proof
Q1	Please confirm that given names and surnames have been identified correctly.
Q2	Please check the citation of Eqs. (35) and (36) is okay as given.
Q3	Please note that Fig. 4 will appear in B/W in print and color in the web version. Based on this, please approve the footnote 1 which explains this.
Q4	Part labels 'a and b' mentioned in the artwork of Figs. 2 and 6 but not in the caption. Please check.
Q5	Part label 'a' mentioned in the artwork of Fig. 3 but not in the caption. Please check.

Please check this box if you have no corrections to make to the PDF file ☐

Thank you for your assistance.

Highlights

▶ Derivations of critical boundaries for system stability in terms of injection impedance. ▶ Derivations of characteristic curves of constant *P*, *Q*, *V* and delta in injection impedance plane. ▶ Example of how one of the derived mappings provides an analytical load flow solution.

Electrical Power and Energy Systems xxx (2012) xxx–xxx

Contents lists available at SciVerse ScienceDirect

Electrical Power and Energy Systems

journal homepage: www.elsevier.com/locate/ijepes

Identification of critical transmission limits in injection impedance plane

Hjörtur Jóhannsson*, Jacob Østergaard, Arne Hejde Nielsen

Centre for Electric Technology, Department of Electrical Engineering, Technical University of Denmark, Elektrovej 325, 2800 Kgs. Lyngby, Denmark

ARTICLE INFO

Article history:
Received 4 September 2010
Received in revised form 22 May 2012
Accepted 24 May 2012
Available online xxxx

Keywords:
Power systems
Security assessment
Stability assessment

ABSTRACT

In this paper, equations are derived that describe the mapping of critical boundaries and characteristic curves from the three dimensional PQV-surface into the two-dimensional injection impedance plane (load impedance plane for both positive and negative resistance). The expressions derived for the critical and characteristic curves in the impedance plane form the basis for a new phasor measurement based situational awareness method, which uses the results in this paper to identify critical operational boundaries in real time and to visualize the system operating conditions in an informative way. The situational awareness method will be described in a later paper, where this paper focuses on the derivations of some system characteristics in the injection (or load) impedance plane. The critical curves from the PQV-surface that are mapped into the impedance plane are the ones representing the conditions where the partial derivatives of the variables P, Q and V in respect to each other become zero. In addition to the mapping of the critical curves, some characteristic curves are mapped as well. These include the mapping of the curves of constant P, Q, V and δ from the PQV-surface into the impedance plane. All of the mapped critical and characteristic curves appear as circles in the injection impedance plane.

1. Introduction

As a consequence of world wide increased political focus on climate changes and thereby an increased focus on reduction of CO_2 emission, it is anticipated that the share of electric power production that is based on renewable energy sources will continually increase in the coming decades. This trend is apparent in many countries where especially power production based on wind and solar energy have been rapidly increasing during the last decade.

In a power system where the share of power production by means of uncontrollable renewable energy sources (such as wind or solar energy) is gradually increasing, the power production becomes more decentralized where the production units are often relatively small and spread over a wide area in the power system. In systems where the amount of wind power production has been significantly increased, the existing transmission system is not always designed to cope with the new production patterns. In many cases, it would be desirable to strengthen existing transmission system, but due to an increasing political and public resistance against further expansion of high voltage transmission grids, future expansions could possible be limited.

Another possibility, instead of strengthening the current transmission system, would be an operation of the existing power system closer to its critical boundaries. Such system operation requires a trustworthy online monitoring of these boundaries. The formation of the power system towards increasing utilization of uncontrollable sources of renewable energy combined with generally more stressed transmission system, necessitates a research within the field of methods providing situational awareness for the power system operation in real time. A situational awareness involves both a knowledge concerning the current operating point, its distance to critical operational boundaries and knowledge of how the operating point could be controlled to increase distance from the critical boundaries.

With the introduction of phasor measurement units (PMUs) [1,2], synchronized measurements of the system voltage and current phasors became possible. With a widespread usage of PMUs in electric power system, a time synchronized snapshots of the system conditions can be updated with a repetition rate equal the system frequency. Several approaches for optimal PMU placement to obtain full observability of the system conditions have been reported [3–5]. The high repetition frequency of PMUs measurements opens up for the development of new applications of wide-area monitoring, detection, protection and control [6–12]. Present and potential applications of phasor measurements have been documented in several surveys [13–15].

One potential application of phasor measurements is to utilize them for obtaining real time situational awareness, where the system stability boundaries are monitored in realtime. As a part of the process of developing methods that assess system stability in real time, it can be useful to express critical system boundaries in terms of measurable system quantities, such as system injection

* Corresponding author.
E-mail addresses: hj@elektro.dtu.dk (H. Jóhannsson), joe@elektro.dtu.dk (J. Østergaard), ahn@elektro.dtu.dk (A.H. Nielsen).

0142-0615/$ - see front matter © 2012 Published by Elsevier Ltd.
http://dx.doi.org/10.1016/j.ijepes.2012.05.050

impedances (the term injection impedance is used to denote a load impedance where the resistive part can be positive or negative). Expressing the system boundaries in the injection impedance plane, real time measurements of the injection impedances can be held against the boundaries, hence providing an assessment of the system stability.

This paper describes analytical derivations for the mapping of some useful characteristics of a three dimensional PQV-surface into an injection impedance plane. The presented expressions for the characteristic boundaries form the basis of a situational awareness method that exploits results from this paper for real time stability assessment and informative visualization of observed system conditions.

2. Critical curves on a PQV-surface

The two bus system and the relevant notations for system variables used in the following derivations are provided in Fig. 1. The relationship between receiving and sending end voltage (E and V), active power P and reactive power Q can be written as:

$$V^4 + V^2(2(RP + XQ) - E^2) + (R^2 + X^2)(P^2 + Q^2) = 0 \quad (1)$$

A solution for either P, Q or V has to be determined if a PQV-surface is to be plotted. Rearranging (1) and solving for P gives the two solutions below:

$$P_{[1]} = -\frac{RV^2 - \sqrt{-Q^2(R^2+X^2)^2 + (R^2+X^2)(E^2 - 2QX)V^2 - X^2V^4}}{R^2+X^2} \quad (2)$$

$$P_{[2]} = -\frac{RV^2 + \sqrt{-Q^2(R^2+X^2)^2 + (R^2+X^2)(E^2 - 2QX)V^2 - X^2V^4}}{R^2+X^2} \quad (3)$$

Letting $R \geqslant 0$ and $X > 0$, then $P_{[2]}$ represents a solution where P is always negative while $P_{[1]}$ represents values of P that can be positive as well as negative. All possible positive values of P are hence described by $P_{[1]}$, given the constrains for R and X considered above.

The entire PQV-surface is described by the two solutions $P_{[1]}$ and $P_{[2]}$. By defining a region S that contains all points on the PQV-surface and subregions S_1 and S_2 that contain the solutions of $P_{[1]}$ and $P_{[2]}$ respectively, then $S = S_1 \cup S_2$ is valid.

Similarly, by manipulating (1) expressions for Q and V can be written as:

$$Q_{[1]} = -\frac{XV^2 + \sqrt{-P^2(R^2+X^2)^2 + (R^2+X^2)(E^2 - 2RP)V^2 - R^2V^4}}{R^2+X^2} \quad (4)$$

$$Q_{[2]} = -\frac{XV^2 - \sqrt{-P^2(R^2+X^2)^2 + (R^2+X^2)(E^2 - 2RP)V^2 - R^2V^4}}{R^2+X^2} \quad (5)$$

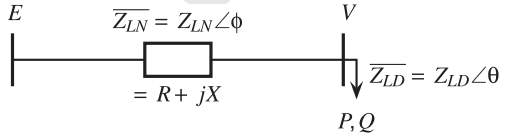

Fig. 1. The simple two bus system and the notations of relevant system variables used in the paper. E and V are sending and receiving end voltage magnitudes respectively, P and Q are active and reactive power at the receiving end, $\overline{Z_{LN}}$ and $\overline{Z_{LD}}$ are line and injection impedance respectively.

$$V_{[1]} = \sqrt{-(RP + XQ) + \frac{E^2}{2} + \sqrt{\frac{E^4}{4} - (XP - RQ)^2 - E^2(RP + XQ)}} \quad (6)$$

$$V_{[2]} = \sqrt{-(RP + XQ) + \frac{E^2}{2} - \sqrt{\frac{E^4}{4} - (XP - RQ)^2 - E^2(RP + XQ)}} \quad (7)$$

$$V_{[3-4]} = -\sqrt{-(RP + XQ) + \frac{E^2}{2} \pm \sqrt{\frac{E^4}{4} - (XP - RQ)^2 - E^2(RP + XQ)}} \quad (8)$$

There are two solutions for Q and four solutions for V. The solutions $V_{[3-4]}$ give negative values for V which has no physical meaning and are therefore not of interest in the following. The solutions $V_{[1-2]}$ result in positive values for V, and are used in the following derivations.

If the regions S_3 and S_4 represent the set of points described by $Q_{[1]}$ and $Q_{[2]}$ respectively and the regions S_5 and S_6 represent the set of points described by $V_{[1]}$ and $V_{[2]}$ respectively, then the equalities $S = S_3 \cup S_4 = S_5 \cup S_6$ are valid.

The expressions provided in (2)–(6) can be used to visualize the relationship between P,Q and V as a three dimensional surface. Such surfaces are depicted in Fig. 2 where the values $E = 1$, $X = 0.1$ and $R = 0.01$ are used. Both surfaces are plotted for positive values of P.

On the surface in Fig. 2a several curves of constant load power factor θ are shown. Projecting these curves onto the PV-plane gives the traditional nose curves (PV-curves), which are often used in voltage stability analysis. Curves of constant receiving end power P are plotted onto the surface in Fig. 2b. Projecting the curves of constant P onto the QV-plane gives the QV-curves, which are as well commonly used for voltage stability analysis. The resulting PV-curves and PQ-curves from the surfaces in Fig. 2a and b are depicted in Fig. 3a and b respectively.

Besides the curves of constant power factor θ and constant power P, two curves of critical importance for stability studies are depicted as well. The first curve intercepts the curves of constant power factor θ when P is at maximum and represents the conditions where the partial derivative $\frac{\partial P}{\partial V}$ is zero. The second curve represents conditions where $\frac{\partial P}{\partial Q} = 0$.

Both curves represent limits for maximum deliverable power P for different system condition. The curve $\frac{\partial P}{\partial V} = 0$ represents maximum deliverable power P when the sending end voltage E is fixed and the relationship between P and Q is linear (that is changes in P are proportional to changes in Q). The curve represents as well the condition for maximum deliverable power P when the value for the reactive power Q is constant.

The curve $\frac{\partial P}{\partial Q} = 0$ represents the maximum deliverable power P when the sending and receiving end voltages (E and V) are constant. The curve could be used as boundary for the maximum deliverable power between two busses, where the voltage at each bus is kept constant. This boundary may be relevant for rotor angle stability as the boundary represents the conditions for maximum power P that a source of constant voltage magnitude can inject into the system. The curve described by $\frac{\partial P}{\partial V} = 0$ represents the situation when the maximum deliverable power P to the load is reached for a fixed load factor θ and is of interest in voltage stability studies.

With regard to the development of real time stability assessment methods, it might be of interest to monitor an instantaneous operating point and determine its margin from the critical boundaries where the partial derivatives in Fig. 2 become zero. Monitoring and visualizing multiple operating points on a PQV-surface is not convenient as the shape of a PQV-surface is dependent on the value of $\overline{Z}_{LN}$ associated with each operating point. On the other hand, a mapping of the main characteristics of a PQV-surface into an injection impedance plane enables the monitoring of multiple operating

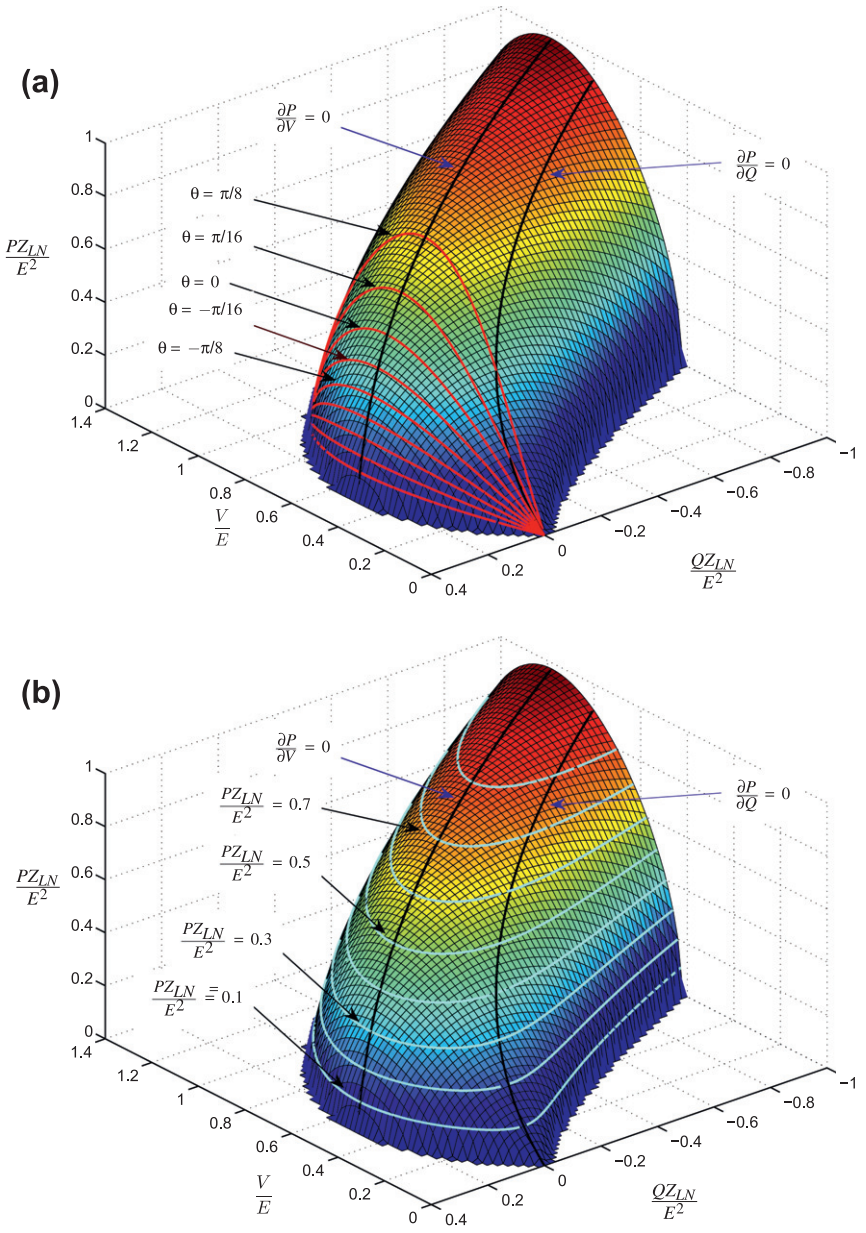

Fig. 2. Relationship between P, Q and V when the sending end voltage E and the line parameters are constant. Above, curves of constant power factor are shown for different values load angle θ. Below, curves of constant power P are shown on same PQV-surface. Fig. 3 shows the projection of these curves onto the PV-plane and the VQ-plane respectively. Curves where the partial derivatives $\partial P/\partial V$ and $\partial P/\partial Q$ become zero are depicted as well.

points since it enables normalization of the monitored operating points in such a way that the same critical boundaries apply to all points. Before mappings of characteristic curves from the PQV-surface can be described, it is necessary to identify some important equalities that enable an analytical derivation of the mappings.

3. Characteristics of the surface

As necessary background for the mapping of the critical curves on the PQV-surface into the injection impedance plane, the following relationship must be valid:

$$\text{When } \frac{\partial P}{\partial V} = 0, \quad \text{then } \frac{\partial Q}{\partial V} = 0. \tag{9}$$

$$\text{When } \frac{\partial P}{\partial Q} = 0, \quad \text{then } \frac{\partial V}{\partial Q} = 0. \tag{10}$$

$$\text{When } \frac{\partial Q}{\partial P} = 0, \quad \text{then } \frac{\partial V}{\partial P} = 0. \tag{11}$$

In the following subsections it is shown that (9)–(11) are valid statements.

3.1. Proof of when $\partial P/\partial V = 0$ then $\partial Q/\partial V = 0$

Differentiating the expression for $P_{[1]}$ in (2) with respect to V yields:

$$\frac{\partial P}{\partial V} = -\frac{2RV}{R^2+X^2} + \frac{V(E^2-2QX)(R^2+X^2)-2X^2V^3}{(R^2+X^2)\sqrt{-Q^2(R^2+X^2)^2+(R^2+X^2)(E^2-2QX)V^2-X^2V^4}} \tag{12}$$

Setting $\frac{\partial P}{\partial V} = 0$ and solving for Q results in:

$$Q_{(\partial P/\partial V=0)} = \frac{X(E^2-2V^2) \pm ER\sqrt{4V^2-E^2}}{2(R^2+X^2)} \tag{13}$$

If $P_{[2]}$ is used instead of $P_{[1]}$ when determining the partial derivative in (12), the same expression for Q as in (13) would be obtained. The result in (13) reveals two solutions for Q, that describe the curve where $\partial P/\partial V = 0$.

It can be seen that (13) is valid for V in the range $[E/2, \infty]$. An description of the entire PQV-surface can be obtained from Eqs.

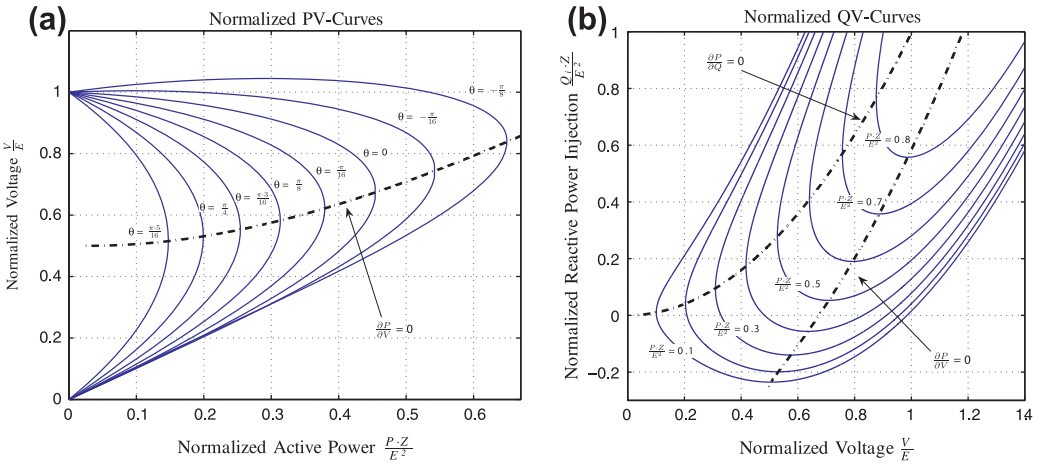

Fig. 3. PV-curves and QV-curves resulting from a projection of the curves of constant power factor in Fig. 2a onto the PV-plane and the projection of the curves of constant power in Fig. 2b onto the QV-plane. Note that *y*-axis in (b) shows the reactive power injection Q_i and has therefore opposite sign to Q in Fig. 2b.

(2) and (3), which correspond to the subregions S_1 and S_2 respectively. Inspection of (13) reveals that the solution with the negative sign lays entirely in S_1 while the solution with the positive sign lays partially in S_1 and S_2. The values of $Q_{(\partial P/\partial V=0)}$ obtained by the solution with the positive sign should therefore be applied into $P_{[1]}$ when the voltage V is in the range $[E/2, E/(2\sin\phi)]$ and applied into $P_{[2]}$ when V is in the range $[E/2\sin\phi, \infty[$. If the values of $Q_{(\partial P/\partial V=0)}$ are not applied in $P_{[1]}$ and $P_{[2]}$ as described, then they do not represent the set of points on the PQV-surface where $\partial P/\partial V = 0$.

The aim is to show that when $\frac{\partial P}{\partial V}=0$ then $\frac{\partial Q}{\partial V}=0$. Differentiation of the expression for $Q_{[1]}$ in (4) in respect to V results in:

$$\frac{\partial Q}{\partial V} = -\frac{2XV}{R^2+X^2} - \frac{V(E^2-2PR)(R^2+X^2)-2R^2V^3}{(R^2+X^2)\sqrt{-P^2(R^2+X^2)^2+(R^2+X^2)(E^2-2PR)V^2-R^2V^4}} \tag{14}$$

Setting $\partial Q/\partial V = 0$ and solving for P results in:

$$P_{(\partial Q/\partial V=0)} = \frac{R(E^2-2V^2) \pm EX\sqrt{4V^2-E^2}}{2(R^2+X^2)} \tag{15}$$

The results are the same as the one that would be obtained if $Q_{[2]}$ would have been used instead of $Q_{[1]}$ in (14).

An analysis of the two solutions for $P_{(\partial Q/\partial V=0)}$ reveals that the expression is valid for V in the range $[E/2, \infty[$. By inspection of the solutions for (15) it can be seen that the solution with the positive sign lays entirely in the region S_1 while the solution with the positive sign lays partially in S_1 and S_2. The values of $P_{(\partial Q/\partial V=0)}$ obtained by the solution with the negative sign represent points in S_1 when the voltage V is in the range $[E/2, E/(2\sin\phi)]$ and represent points in S_2 when V is in the range $[E/(2\sin\phi), \infty[$.

By constraining expression for $P_{[1]}$ in (2) by inserting the expression with the positive sign for $Q_{(\partial P/\partial V=0)}$ in (13) (which lays entirely in S_1) gives:

$$\begin{aligned} P &= \frac{-2RV^2+\sqrt{2XE^2\sqrt{R^2E^2(2V-E)(2V+E)}+E^4R^2+4X^2V^2E^2-X^2E^4}}{2(R^2+X^2)} \\ &= \frac{-2RV^2+E\sqrt{(RE+X\sqrt{(2V-E)(2V+E)})^2}}{2(R^2+X^2)} \\ &= \frac{R(E^2-2V^2)+EX\sqrt{4V^2-E^2}}{2(R^2+X^2)} \end{aligned} \tag{16}$$

The above expression for P, which is constrained by $\partial P/\partial V = 0$, is the same as the expression for P with the positive sign in (15) where $\partial Q/\partial V = 0$. It is therefore proven that the curve on the surface where $\partial Q/\partial V = 0$ is the same curve as the one where $\partial P/\partial V = 0$.

3.2. Proof of when $\partial P/\partial Q = 0$ then $\partial V/\partial Q = 0$

Differentiation of the expression for $P_{[1]}$ in (2) with respect to Q yields:

$$\frac{\partial P}{\partial Q} = \frac{-Q(R^2+X^2)-XV^2}{\sqrt{-Q^2(R^2+X^2)^2+(R^2+X^2)(E^2-2QX)V^2-X^2V^4}} \tag{17}$$

Setting $\partial P/\partial Q = 0$ and solving for Q yields:

$$Q_{(\partial P/\partial Q=0)} = -\frac{XV^2}{R^2+X^2} \tag{18}$$

This result would be obtained as well if $P_{[2]}$ is differentiated in (17) instead of $P_{[1]}$. By inspecting the expressions for $Q_{[1]}$ and $Q_{[2]}$ in (4) and (5) it can be seen that the expression for $Q_{(\partial P/\partial Q=0)}$ is identical to $Q_{[1]}$ and $Q_{[2]}$ when the term under the root equals zero. This means that the curve representing $\partial P/\partial Q = 0$ is at the boundary of regions described by $Q_{[1]}$ and $Q_{[2]}$ (S_3 and S_4 respectively). Therefore, the expression for $Q_{(\partial P/\partial Q=0)}$ represents the intersection between $Q_{[1]}$ and $Q_{[2]}$ ($Q_{(\partial P/\partial Q=0)} = S_3 \cap S_4$). This results in that (18) is valid for all values of V in both expressions of $Q_{[1]}$ and $Q_{[2]}$ in (4) and (5) respectively.

The aim of this subsection is to show that when $\partial P/\partial Q = 0$ then $\partial V/\partial Q = 0$. Expressions for the positive voltage magnitudes ($V_{[1]}$ and $V_{[2]}$) were derived in (6) and (7). Differentiation of the expression for $V_{[1]}$ in respect to Q yields:

$$\frac{\partial V}{\partial Q} = \frac{2R(XP-RQ)-E^2X-X\sqrt{d}}{\sqrt{2d\sqrt{d}+2d(E^2-2(RP+QX))}} \tag{19}$$

where $d = -4(RQ-XP)^2 + E^2(E^2-4(RP+QX))$. Setting $\partial V/\partial Q = 0$ and solving for P results in:

$$P_{(\partial V/\partial Q=0)} = \frac{RQ \pm E\sqrt{-QX}}{X} \tag{20}$$

This expression would have been obtained as well, if any one of the four solutions for the voltages ($V_{[1-4]}$ in (6)–(8)) would have been differentiated in (19) and used to determine $P_{(\partial V/\partial Q=0)}$. Eq. (20) is valid for negative Q when X is positive (inductive) and vice versa.

To show that $\partial P/\partial Q = 0$ and $\partial V/\partial Q = 0$ are identical, the expression for $Q_{(\partial P/\partial Q=0)}$ from (18) is put into the expression for $P_{[1]}$ given by (2). Doing so gives:

$$P_{[1]} = \frac{\left(-RV + \sqrt{R^2E^2 + X^2E^2}\right)V}{R^2 + X^2} \tag{21}$$

This expression can be achieved by inserting $Q_{(\partial P/\partial Q=0)}$ from (18) into the expression for $P_{(\partial V/\partial Q=0)}$ with the positive sign given by (20):

$$\begin{aligned} P_{(\partial V/\partial Q=0)} &= \frac{RQ_{(\partial P/\partial Q=0)} + E\sqrt{-Q_{(\partial P/\partial Q=0)}X}}{X} \\ &= \frac{(-RV + \sqrt{R^2E^2 + X^2E^2})V}{R^2 + X^2} \end{aligned} \tag{22}$$

Since the same result is obtained by constraining the surface described by $P_{[1]}$ with $Q_{(\partial P/\partial Q= 0)}$ as by constraining the curve described by $P_{(\partial V/\partial Q=0)}$ with $Q_{(\partial P/\partial Q=0)}$, it is proven that the curve on the surface where $\partial V/\partial Q = 0$ is the same as the curve where $\partial P/\partial Q = 0$.

3.3. Proof of when $\partial Q/\partial P = 0$ then $\partial V/\partial P = 0$

Differentiation of the expression for $Q_{[1]}$ in (4) with respect to P yields:

$$\frac{\partial Q}{\partial P} = \frac{RV^2 + P(R^2 + X^2)}{\sqrt{-P^2(R^2 + X^2)^2 + (V^2E^2 - 2V^2RP)(R^2 + X^2) - R^2V^4}} \tag{23}$$

Rearranging and solving for P, when $\frac{\partial Q}{\partial P} = 0$ results in.

$$P_{(\partial Q/\partial P=0)} = -\frac{RV^2}{R^2 + X^2} \tag{24}$$

This is the same result as would have been obtained if $Q_{[2]}$ in (5) would have been differentiated in (23) instead of $Q_{[1]}$. Inspection of Eqs. (2) and (3) for $P_{[1]}$ and $P_{[2]}$ respectively, reveals that $P_{(\partial Q/\partial P=0)}$ is identical to $P_{[1]}$ and $P_{[2]}$ when the term under the root equals zero. This means that the curve representing $\partial Q/\partial P = 0$ is at the boundaries of $P_{[1]}$ and $P_{[2]}$ ($\partial Q/\partial P = 0$ at $S_1 \cap S_2$). Therefore, (24) is valid for all values of V in either $P_{[1]}$ or $P_{[2]}$.

The aim is to show that when $\partial Q/\partial P = 0$ then $\partial V/\partial P = 0$. Differentiating the expression for $V_{[1]}$ in (6) in respect to P yields:

$$\frac{\partial V}{\partial P} = \frac{2X(RQ - XP) - E^2R - R\sqrt{d}}{\sqrt{2d\sqrt{d}) + 2d(E^2 - 2(RP + QX))}} \tag{25}$$

where $d = -4(RP - QX)^2 + E^2(E^2 - 4(RP + QX))$.

Rearranging and solving for Q, when $\frac{\partial V}{\partial P} = 0$ results in.

$$Q_{(\partial V/\partial P=0)} = \frac{PX \pm E\sqrt{-RP}}{R} \tag{26}$$

If any one of the four solutions for the voltages ($V_{[1-4]}$ in (6)–(8)) would have been differentiated in (25) and used to determine $Q_{(\partial V/\partial P=0)}$, the same expression is obtained. Eq. (26) is valid for negative P if R is positive and vice versa.

Inserting the expression for $P_{(\partial Q/\partial P=0)}$ form (24) into the expressions for $Q_{[1]}$ and $Q_{[2]}$ in (4) and (5) yields:

$$Q_{[1]} = -\frac{XV^2 + EV\sqrt{R^2 + X^2}}{R^2 + X^2} \tag{27}$$

$$Q_{[2]} = -\frac{XV^2 - EV\sqrt{R^2 + X^2}}{R^2 + X^2} \tag{28}$$

Same results would be obtained if the expression for $Q_{(\partial V/\partial P=0)}$ in (26) would have been constrained by inserting $P_{(\partial Q/\partial P=0)}$ from (24). This proves that the curve on the PQV-surface where $\partial Q/\partial P = 0$ is the same as the curve where $\partial V/\partial P = 0$.

4. Transformation of the critical curves into injection impedance plane

The following sections describe the mapping of the curves on the PQV-surface, that represent the set of points where the partial derivatives become zero, into the injection impedance plane.

4.1. Transformation of the curve that represents $\partial P/\partial Q = \partial V/\partial Q = 0$ into injection impedance plane

By writing the expression for $Q_{(\partial P/\partial Q=0)}$ from (18) in terms of apparent injection impedance Z_{LD} results in:

$$Q_{(\partial P/\partial Q=0)} = -\frac{XV^2}{R^2 + X^2} = \frac{V^2 \sin\theta}{Z_{LD}} \tag{29}$$

and solving for Z_{LD} results in:

$$Z_{LD} = -\frac{Z_{LN} \sin\theta}{\sin\phi} \tag{30}$$

From (30) it can be seen that the curve that represents $\partial P/\partial Q = \partial V/\partial Q = 0$ is mapped as a circle in the injection impedance plane. The circle intercepts the origin of the plane, the complex conjugate of the line impedance and the negative of the line impedance. That is, the curve where $\partial P/\partial Q = \partial V/\partial Q = 0$ appears as a circle with center in the impedance plane at ($R_{LD} = 0, X_{LD} = -r$) where r is the radius of the circle and can be expressed as:

$$r = \frac{Z_{LN}}{2\sin\phi} \tag{31}$$

4.2. Transformation of the curve that represents $\partial Q/\partial P = \partial V/\partial P = 0$ into injection impedance plane

Revisiting the expression for $P_{(\partial Q/\partial P=0)}$ in (24), which satisfies the conditions $\partial Q/\partial P = \partial V/\partial P = 0$, and equating it to an expression for P in terms of apparent injection impedance Z_{LD} results in:

$$P = -\frac{RV^2}{R^2 + X^2} = \frac{V^2 \cos\theta}{Z_{LD}} \tag{32}$$

and solving for Z_{LD} yields:

$$Z_{LD} = -\frac{Z_{LN} \cos\theta}{\cos\phi} \tag{33}$$

From (33) it can be seen that the curve that represents $\partial Q/\partial P = \partial V/\partial P = 0$ is mapped as a circle in the injection impedance plane. The circle intercepts the origin of the plane, the real conjugate of the line impedance and the negative of the line impedance. That is, the curve where $\partial Q/\partial P = \partial V/\partial P = 0$ appears as a circle with center in the impedance plane at ($R_{LD} = -r, X_{LD} = 0$) where r is the radius of the circle and is expressed as:

$$r = \frac{Z_{LN}}{2\cos\phi} \tag{34}$$

4.3. Transformation of the curve that represents $\partial P/\partial V = \partial Q/\partial V = 0$ into injection impedance plane

Previously, it was shown that the expression for $P_{(\partial Q/\partial V=0)}$ in (15) and the expression for $Q_{(\partial P/\partial V=0)}$ in (13) describe the same curve on the PQV-surface where $\partial P/\partial V = \partial Q/\partial V = 0$.

Furthermore, it was stated in Section 3.1 that the solution for $P_{(\partial Q/\partial V=0)}$ with the negative sign lies entirely on the same surface as the solution of $Q_{(\partial P/\partial V=0)}$ with the positive sign. By rewriting and manipulating the solutions for $P_{(\partial Q/\partial V=0)}$ and $Q_{(\partial P/\partial V= 0)}$ that lie on the same surface gives:

$$P_{(\partial Q/\partial V=0)} = \frac{R(E^2-2V^2) - XE\sqrt{4V^2-E^2}}{2(R^2+X^2)} = \frac{RA-XB}{C} \quad (35)$$

$$Q_{(\partial P/\partial V=0)} = \frac{X(E^2-2V^2) + RE\sqrt{4V^2-E^2}}{2(R^2+X^2)} = \frac{XA+RB}{C} \quad (36)$$

where $A = (E^2 - 2V^2)$, $B = E\sqrt{4V^2 - E^2}$ and $C = 2(R^2 + X^2)$. The aim is to derive an expression for the curve where $\partial P/\partial V = \partial Q/\partial V = 0$. For that purpose, the following relationship is utilized:

$$\left(\frac{V^2}{Z_{LD}}\right)^2 = P^2 + Q^2 \quad (37)$$

Inserting the expressions for P and Q in (35) and (36) into the above equation gives:

$$\left(\frac{V^2}{Z_{LD}}\right)^2 = \frac{R^2A^2 - 2RXAB + X^2B^2}{C^2} + \frac{X^2A^2 + 2RXAB + R^2B^2}{C^2} = \frac{(R^2+X^2)(A^2+B^2)}{C^2} = \frac{(A^2+B^2)}{4(R^2+X^2)} = \frac{V^4}{Z_{LN}^2} \quad (38)$$

and solving for Z_{LD} results in:

$$Z_{LD} = Z_{LN} \quad (39)$$

Hence, the set of points on the PQV-surface that describe $\partial P/\partial V = \partial Q/\partial V = 0$ appear as a circle in the injection impedance plane with center at the origin and radius equal to the magnitude of $\overline{Z_{LN}}$. This was an expected result and is in accordance with the well known maximum power transfer theorem for AC networks.

4.4. Graphical representation of the critical curves in the impedance plane

Fig. 4 shows a plot of the three borderlines of interest. It has been shown that the curve where $\partial P/\partial V = \partial Q/\partial V = 0$ appears as a circle in the impedance plane with its center at the origin and a radius equal the size of the line impedance Z_{LN}. This curve is plotted as a black circle in the impedance plane and it can be said to represent the maximum deliverable power through Z_{LN} when the sending end voltage is maintained fixed as well as θ or Q.

The curve where $\partial P/\partial Q = \partial V/\partial Q = 0$ is plotted as a red[1] circle in the figure. This borderline represents the maximum deliverable power through the line impedance Z_{LN} when both the sending end and the receiving end voltages are fixed. This borderline could be useful in determining the maximum transferrable power between two subsystems where the voltage in each subsystem is maintained constant by local generators.

The third curve shown in Fig. 4 (green line) represents the situation where $\partial P/\partial Q = \partial V/\partial Q = 0$. This borderline represents the situation where maximum or minimum reactive power is transferred through Z_{LN} when both the sending end and receiving end voltage is fixed. This curve is of limited interest when studying stability in power system.

5. Transformation of other characteristic curves on the PQV-surface into impedance plane

The previously derived mappings of the critical curves where the partial derivatives on the PQV-surface are zero, are useful in stability studies [10]. For the purpose of establishing meaningful visualization of a given operating condition in injection impedance plane, the mapping of curves of constant P, Q, V and δ become of interest. In the following section, the mappings of those curves are derived.

5.1. Curves of constant P

In order to derive expressions for curves of constant P in the injection impedance plane, the expression (6) is used. In order to relate the values of P to Z_{LD}, it is necessary to express V and Q as a function of those variables:

$$V^2 = \frac{Z_{LD}P}{\cos\theta} \quad (40)$$

$$Q = P\tan\theta \quad (41)$$

An expression for values of constant P described as a function of Z_{LD} is obtained by raising (6) in powers of two and inserting the expressions for V^2 and Q from (40) and (41). After manipulation, an expression of Z_{LD} as circle in polar coordinates can be obtained:

$$ZLD = r_0 \cdot \cos(\theta - \varphi) \pm \sqrt{r^2 + r_0^2 \cdot \sin^2(\theta - \varphi)} \quad (42)$$

where

$$r = \sqrt{\frac{E^4 - 4E^2RP}{4P^2}}$$

$$r_0 = \sqrt{X^2 + R^2 + \frac{E^4}{4P^2} - \frac{RE^2}{P}}$$

$$\tan\varphi = \frac{-X}{-\left(R - \frac{E^2}{2P}\right)}$$

The expression in (42) represents the set of points in the injection impedance plane where the receiving end power P is constant. Curves of constant power appear as circles in the injection impedance plane. In the above, r_0 is the distance from the origin to the center of the circle, r is the radius of the circle and φ is the angle between the positive real axis and the line connecting the origin and the center of the circle.

5.2. Curves of constant Q

In order to derive expressions for curves of constant Q in the injection impedance plane, the expression in (6) is used again along with the following expressions for V^2 and Q:

$$V^2 = \frac{Z_{LD}Q}{\sin\theta} \quad (43)$$

$$Q = P\tan\theta \quad (44)$$

Inserting (43) and (44) into the square of (6) and solving for Z_{LD} gives the following expression in polar coordinates:

$$ZLD = r_0 \cdot \cos(\theta - \varphi) \pm \sqrt{r^2 + r_0^2 \cdot \sin^2(\theta - \varphi)} \quad (45)$$

where

$$r = \sqrt{\frac{E^4 - 4E^2XQ}{4Q^2}}$$

$$r_0 = \sqrt{X^2 + R^2 + \frac{E^2}{4Q^2} - \frac{XE}{Q}}$$

$$\tan\varphi = \frac{-\left(X - \frac{E^2}{2Q}\right)}{-R}$$

Eq. (45) represents a circle in the injection impedance or a fixed value of Q. In the above, r_0 is the distance from the origin to the center of the circle, r is the radius of the circle and φ is the angle between

[1] For interpretation of color in Fig. 4, the reader is referred to the web version of this article.

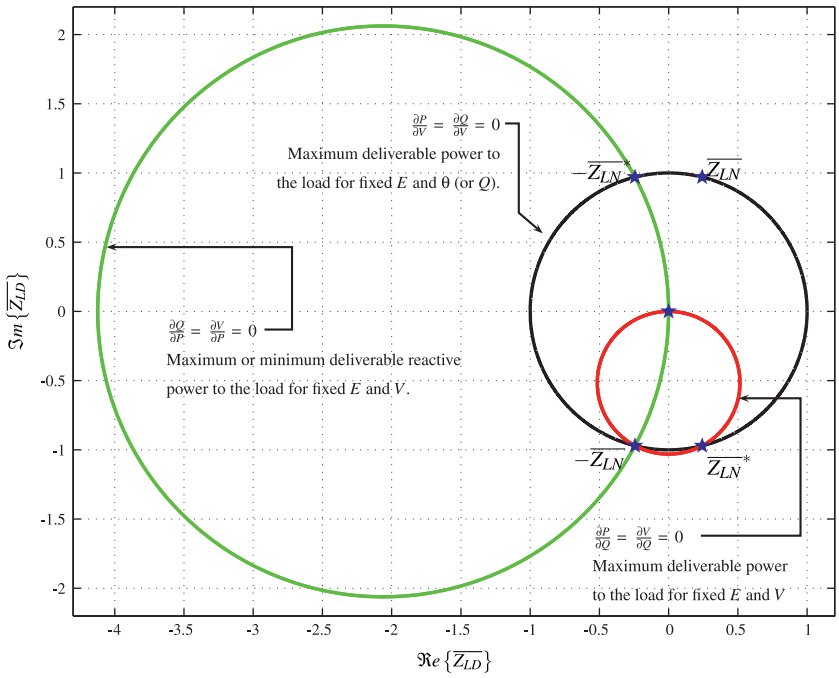

Fig. 4. Graphical representation of the critical lines in the injection impedance plane.

the positive real axis and the line connecting the origin and the center of the circle.

5.3. Curves of constant V

In order to derive expressions for curves of constant V in the injection impedance plane, (3) is used along with the following expressions for P and Q:

$$P = \frac{V^2}{Z_{LD}}\cos\theta \tag{46}$$

$$Q = \frac{V^2}{Z_{LD}}\sin\theta \tag{47}$$

By inserting (46) and (47) into (3) and solving for Z_{LD} results in the following expression in polar coordinates.

$$ZLD = r_0 \cdot \cos(\theta - \varphi) \pm \sqrt{r^2 + r_0^2 \cdot \sin^2(\theta - \varphi)} \tag{48}$$

where

$$r = \frac{EV\sqrt{R^2 + X^2}}{V^2 - E^2}$$

$$r_0 = \frac{V^2\sqrt{R^2 + X^2}}{V^2 - E^2}$$

$$\tan\varphi = \frac{-X}{-R}$$

The curves of constant voltage are represented as circles in the injection impedance plane. As before, r_0 is the distance from the origin to the center of the circle, r is the radius of the circle and φ is the angle between the positive real axis and the line connecting the origin and the center of the circle.

5.4. Curves of constant voltage angel δ

In order to derive expressions for curves of constant bus voltage phase angle δ in the injection impedance plane, the following expressions for P and Q are used:

$$P = \frac{V^2}{Z_{LD}}\cos\theta \tag{49}$$

$$P = \frac{EV\cos(\delta + \phi) - V^2\cos(\phi)}{Z_{LN}} \tag{50}$$

$$Q = \frac{V^2}{Z_{LD}}\sin\theta \tag{51}$$

$$Q = \frac{EV\sin(\delta + \phi) - V^2\sin(\phi)}{Z_{LN}} \tag{52}$$

Setting (49) equal (50) and solving for V results in:

$$V = \frac{EZ_{LD}\cos(\delta + \phi)}{Z_{LN}\cos\theta + Z_{LD}\cos\phi} \tag{53}$$

Similarly, setting (51) equal (52) and solving for V gives:

$$V = \frac{EZ_{LD}\sin(\delta + \phi)}{Z_{LN}\sin\theta + Z_{LD}\sin\phi} \tag{54}$$

Finally, setting (53) equal (54) and solving for Z_{LD} yields:

$$ZLD = -\frac{Z_{LN}}{\sin\delta}\cdot\sin(\delta + \phi - \theta) \tag{55}$$

This equation represents a circle in the injection impedance plane for constant values of δ. The circle represented in (55) has a diameter equal $Z_{LN}/\sin\delta$ and intercepts the origin of the injection impedance plane and the point $Z_{\overline{LD}} = -\overline{Z_{LN}}$ for all values of constant δ.

Each circle obtained from (55) represents the conditions for two different values of constant δ; that is when $\delta = \delta_0$ and when $\delta = -180° + \delta_0$ where δ_0 is arbitrary. Therefore, it has to be investigated which part of the circle represents constant $\delta = \delta_0$ and which part represents constant $\delta = -180° + \delta_0$. For simplicity, it is assumed that $0° \leqslant \delta_0 < 180°$. If $\delta_0 = 0°$, then (55) reveals that the circle representing $\delta = \delta_0$ and $\delta = -180° + \delta_0$ has an radius going towards infinity and these conditions are represented by the straight line that intercepts the origin and the point where $\overline{Z_{LD}} = \overline{Z_{LN}}$. An inspection shows that the part of the line between the two singular points (the origin and the point where $\overline{Z_{LD}} = -\overline{Z_{LN}}$ represents the condition where $\delta = \pm 180°$ while other parts of the line represent conditions where $\delta = 0°$.

If the line intercepting the origin and the point where $\overline{Z_{LD}} = -\overline{Z_{LN}}$ is used to split the impedance plane into two halves, then by inspection it can be shown that all of the circles representing a constant δ lie in both halves. The curves of constant δ, when $\delta = \delta_0$ are represented by the part of the circle laying in the left half plane while the condition where $\delta = -180 + \delta_0$ are represented by the part of the circle laying in the right half plane. Fig. 5 illustrates how the same circle in the impedance plane represents two different conditions of constant phase angle δ, depending on in which half plane the circle parts lie in.

5.5. Graphical representation of the characteristic curves in the impedance plane

Figs. 6 and 7a and b illustrate how curves of constant *P*,*Q*, *V* and δ appear in the injection impedance plane. The figures represent the situation when $\overline{Z_{LN}} = (1\angle\phi)$ and $\phi = 75°$.

Fig. 6a shows how the curves of constant receiving end power *P* appear in the complex injection impedance plane. Inspection of the curves of constant *P*, reveals certain symmetry in how they appear in the impedance plane. Values of constant positive *P* appear as circles in the right half plane and the radius of the circle gradually decreases as the power is increased toward the point of maximum deliverable power. The point of maximum deliverable power is where the injection impedance is equal the complex conjugate of the line impedance. Values of constant negative *P* are represented in the left half pane of the injection impedance plane. The radius of the circles representing constant negative power (positive bus injection) gradually decreases as the absolute value of the power increases. The point of minimum deliverable power (maximum bus injection) occurs at the singular point where the injection impedance is equal to the negative of the line impedance. at this point the receiving end power *P* goes towards $-\infty$. The set of points representing the situation where *P* is zero, appears as a straight line that satisfies $R = 0$.

Fig. 6b shows how the curves of constant *Q* appear in the complex injection impedance plane. The curves for constant *Q* have a similar appearance as curves of constant *P*. The circles for constant positive values of *Q* appear in the upper half plane, where the radius of the circles gradually decreases until the point of maximum positive *Q* is obtained. The point of maximum *Q* occurs when the value of the injection impedance is equal to the real conjugate of the line impedance ($X_{LD} = X_{LN}$ and $R_{LD} = -R_{LN}$). The circles representing negative constant values of *Q* appear in the lower half plane and the minimum occurs at the singular point where the injection impedance is equal the negative of the line impedance. At the singular point, the value of *Q* goes towards $-\infty$. The set of points representing the situation where *Q* is zero, appears as a straight line that satisfies $X = 0$.

Fig. 7a shows how curves of constant *V* appear in the injection impedance plane. It can be seen that the circles representing constant values of *V* have center points on an imaginary line intercepting the origin of the injection impedance plane and the singular point where $\overline{Z_{LD}} = -\overline{Z_{LN}}$. The set of points where $V = E$ appears as straight line that is perpendicular to the same imaginary line and intercepts that line in the point where $\overline{Z_{LD}} = -\overline{Z_{LN}}/2$. The line representing $V = E$ divides the injection impedance plane into to half planes, where values of *V* lower than *E* appear as circles in the half plane containing the origin, while values of *V* greater than *E* appear as circles in the half containing the singular point $\overline{Z_{LD}} = -\overline{Z_{LN}}$.

Fig. 7b shows that the curves of constant voltage phase angle δ appear as circles in the injection impedance plane. All circles intercept the origin and the singular point where $\overline{Z_{LD}} = -\overline{Z_{LN}}$. The part of the circles going in counter clockwise direction from the origin to $Z_{LD} = -Z_{LN}$ represents positive angles of δ (if δ is defined to lie in the range $-180° < \delta \leqslant 180°$) while the part of the circle going in clockwise direction from the origin to $Z_{LD} = -Z_{LN}$ represents the points where δ is negative.

Furthermore, it can be noted that the circle where the partial derivative $\partial P/\partial Q = 0$ is the same as the circle representing fixed δ when $\delta = -\phi$ and $\delta = 180° - \phi$. This means that the point of maximum deliverable *P* to the receiving end in Fig. 1 when *V* and *E* are fixed occurs at $\delta = -\phi$ and the point of minimum deliverable power (maximum injectable power) occurs at $\delta = 180° - \phi$.

Similarly, it can be seen that the circle where the partial derivative $\partial Q/\partial P = 0$ is the same as the circle representing fixed δ when $\delta = -90° - \phi$ and $\delta = 90° - \phi$. This means that the part of the circle where $\delta = -90° - \phi$ represents the points of maximum deliverable *Q* when *V* and *E* are fixed, while $\delta = 90° - \phi$ represents the minimum deliverable *Q* (maximum reactive power injection) for the same conditions.

6. Example – analytical load flow for a two bus system

The derived expressions for the PQV-characteristics can be used to provide an analytical solution of the load flow problem for a simple two bus system. Choosing the sending end as a reference bus, the power flow solution can be analytically determined by

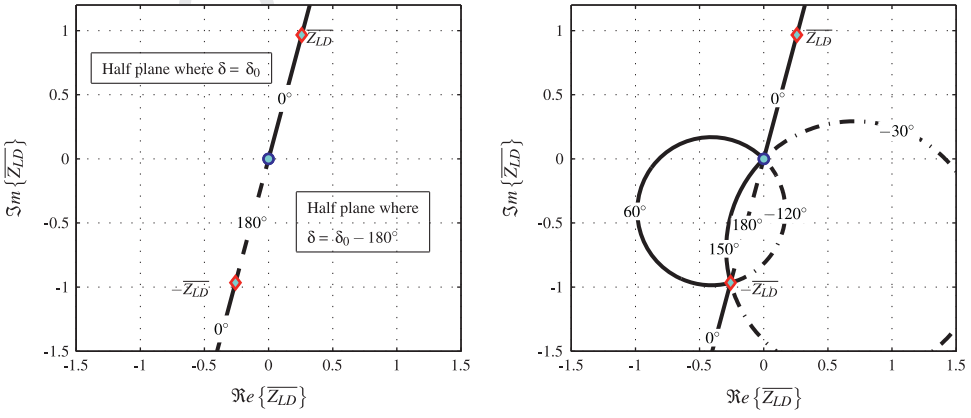

Fig. 5. Curves of constant δ in the injection impedance plane. To the left, a plot of the curve of constant δ for the special case when δ is either 0° or 180°. These values of δ appears as straight line, where the part between the origin and $-\overline{Z_{LD}}$ represents $\delta = \pm 180°$ while other parts represent $\delta = 0°$. To the right, two parts of the same circle represent two different values of constant δ depending of on which side of the line $\delta = 0°$ the parts are located. Defining $0 \leqslant \delta_0 < 180$, then the condition $\delta = \delta_0$ is the part of the circle lying in the left half plane while $\delta = \delta_0 - 180°$ is represented by the same circle, just by the part lying in the right half plane.

Please cite this article in press as: Jóhannsson H et al. Identification of critical transmission limits in injection impedance plane. Int J Electr Power Energ Syst (2012), http://dx.doi.org/10.1016/j.ijepes.2012.05.050

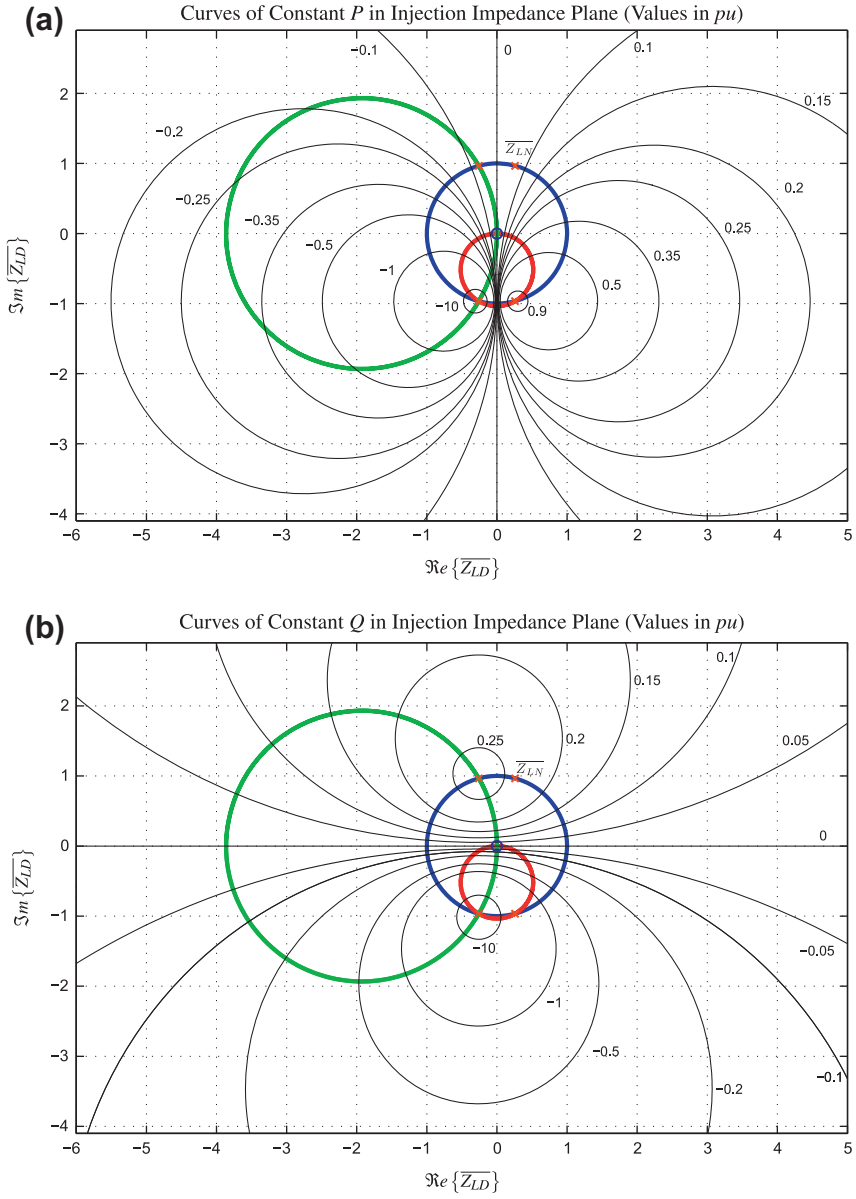

Fig. 6. Curves of constant active and reactive power in the complex injection impedance plane, with $\overline{Z_{LN}} = (1\angle 75^\circ)$. Above, curves for P are shown along with the previously derived curves where the partial derivatives became zero. The values shown are in per unit where $S_{base} = E^2/Z_{LN}$. Curves for positive P appear as circles in the right half plane, where the circle radius decreases as the value of constant P increases until the point of maximum deliverable power is reached (when $\overline{Z_{LD}} = \overline{Z_{LN}}^*$). Circles representing negative P (power injection) lie all in the left half plane where the circles radius decreases as the absolute value of P increases until the singular point where $\overline{Z_{LD}} = -\overline{Z_{LN}}$ is reached (where $P \to -\infty$). Below, curves of constant Q (per unit values) are shown where the curves of constant positive Q are represented as circles in the upper half plane and curves of constant negative Q are represented in the lower half plane. The point of maximum positive Q occurs when $\overline{Z_{LD}} = -\overline{Z_{LN}}^*$ while at the singular point $\overline{Z_{LD}} = -\overline{Z_{LN}}$ the value of Q goes towards $-\infty$.

considering the where the circles of constant P and Q intercept in the injection impedance plane.

Eq. (42) describes the curves of constant P as function of E, R, X and θ. With values of P and Q specified, θ is known and hence the load impedance values corresponding to the load flow solutions can directly be determined from (42). With the load impedance known, the complex receiving end voltage $\overline{V}$ can be determined which provides the load flow solution for the system of concern.

7. Conclusion

Analytical derivation for the mapping of critical and characteristic curves on a three dimensional PQV-surface into the injection plane were introduced in this paper. The critical curves of interest were those where the partial derivative of the variables P, Q and V in respect to each other becomes zero.

The curve satisfying $\partial P/\partial Q = 0$ represents a maximum receivable or injectable power at a bus when the voltage magnitude in both ends is constant. This limit appears as the circle in the impedance plane that intercepts the origin and the points where the injection impedance was equal the negative of the line impedance and equal the complex conjugate of the line impedance. This boundary can become useful for determining the maximum power that a given generator can inject a node of constant steady state voltage magnitude. If an observation of the injection impedance for a given generator crosses these limits, the generator is prone to lose its synchronism with the rest of the system. In fact, the

Please cite this article in press as: Jóhannsson H et al. Identification of critical transmission limits in injection impedance plane. Int J Electr Power Energ Syst (2012), http://dx.doi.org/10.1016/j.ijepes.2012.05.050

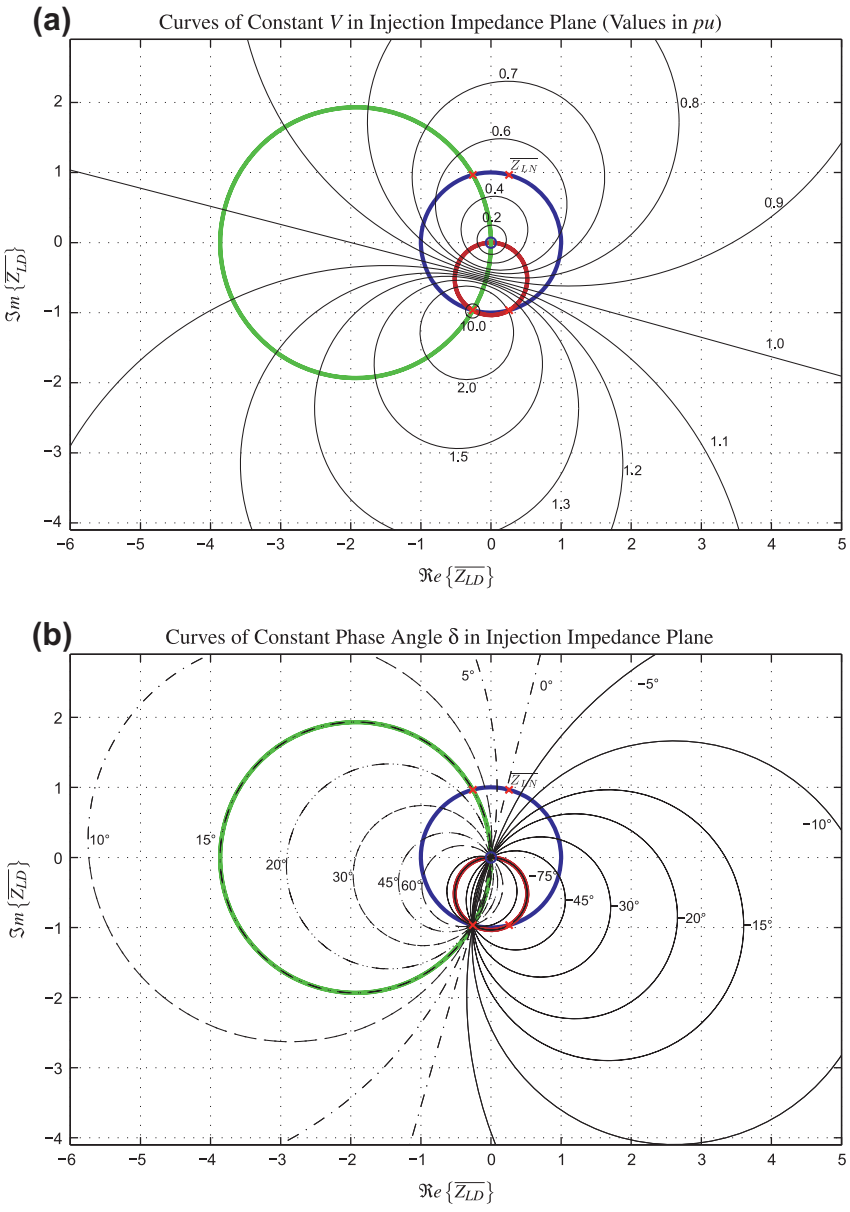

Fig. 7. Curves of constant voltage magnitude V and voltage phase angle δ, when $\overline{Z_{LN}} = Z_{LN}\angle\phi = 1\angle 75^{\circ}$. (a) Curves of constant V in per unit where sending end voltage E is used as base value. The straight line where E and V are equal (V = 1.0 pu) divides the plane in two half planes, one plane containing the origin of the injection impedance plane, the other plane containing the singular point $\overline{Z_{LD}} = -\overline{Z_{LN}}$. Curves of constant V when V < 1.0 pu, appear as circles that encapsulate the origin while curves of constant V when V > 1.0 pu, appear as circles encapsulating the point $\overline{Z_{LD}} = -\overline{Z_{LN}}$. The origin represent the point where V = 0 while at the singular point $\overline{Z_{LD}} = -\overline{Z_{LN}}$, V approaches ∞. (b) Curves of constant δ that appear as well as circles. All of the circles intercepts the origin and the point $\overline{Z_{LD}} = -\overline{Z_{LN}}$. The critical curve where $\partial P/\partial Q$ = 0 is the same circle as where $\delta = [-\phi, 180 - \phi]$ and the circle representing $\partial Q/\partial P$ = 0 is the same as the circle where $\delta = [90 - \phi, -90 - \phi]$.

boundary satisfying $\partial P/\partial Q = 0$ plays an central role in a real time stability assessment application to be described in a later publication.

The mapping of characteristic curves into the injection impedance plane are useful when an information a bout a given system condition is to be visualized in a real time application. The knowledge of how critical operational boundaries and other characteristic curves appear in the impedance plane is useful for obtaining a situational awareness for a given operating condition. The derived curves can illustrate where stability and operational boundaries are located in respect to the observed operating point. In that way an information concerning distance to boundaries of critical operation can be visualized in real time.

Furthermore, the analytical derivation of critical stability boundaries in the impedance plane enables a normalization of multiple operating points in such a way that the same critical boundary applies to all of the normalized points. This results in that multiple operating points can be visualized on the same screen and held against the same normalized stability boundary.

References

[1] Phadke A. Synchronized phasor measurements in power systems. IEEE Comput Appl Power 1993;6(2):10–5.
[2] Phadke A, Thorp J. Synchronized phasor measurements and their applications. Springer Verlag; 2008.
[3] Jamuna K, Swarup K. Optimal placement of PMU and SCADA measurements for security constrained state estimation. Int J Electr Power Energy Syst 2011;33(10):1658–65.
[4] Hajian M, Ranjbar AM, Amraee T, Mozafari B. Optimal placement of PMUS to maintain network observability using a modified BPSO algorithm. Int J Electr Power Energy Syst 2011;33(1):28–34.

Please cite this article in press as: Jóhannsson H et al. Identification of critical transmission limits in injection impedance plane. Int J Electr Power Energ Syst (2012), http://dx.doi.org/10.1016/j.ijepes.2012.05.050

[5] Roy BS, Sinha A, Pradhan A. An optimal PMU placement technique for power system observability. Int J Electr Power Energy Syst 2012;42(1):71–7.
[6] Glavic M, Van Cutsem T. Wide-area detection of voltage instability from synchronized phasor measurements. Part I: Principle. IEEE Trans Power Syst 2009;24(3):1408–16.
[7] Glavic M, Van Cutsem T. Wide-area detection of voltage instability from synchronized phasor measurements. Part II: Simulation results. IEEE Trans Power Syst 2009;24(3):1417–25.
[8] Milosevic B, Begovic M. Voltage-stability protection and control using a wide-area network of phasor measurements. IEEE Trans Power Syst 2003;18(1):121.
[9] Kakimoto N, Sugumi M, Makino T, Tomiyama K. Monitoring of interarea oscillation mode by synchronized phasor measurement. IEEE Trans Power Syst 2006;21(1).
[10] Jóhannsson H, Garcia-Valle R, Weckesser J, Nielsen A, Østergaard J. Real-time stability assessment based on synchrophasors. In: Proceedings of the 2011 IEEE Trondheim PowerTech. IEEE; 2011.
[11] Gu W, Wan Q. Linearized voltage stability index for wide-area voltage monitoring and control. Int J Electr Power Energy Syst 2010;32(4):333–6.
[12] Zhang Y, Wang Z, Zhang J, Ma J. Fault localization in electrical power systems: a pattern recognition approach. Int J Electr Power Energy Syst 2011;33(3):791–8.
[13] Novosel D, Madani V, Bhargava B, Vu K, Jim C. Dawn of the grid synchronization. IEEE Power Energy Mag 2008;6(1):49–60.
[14] Phadke AG, Volskis H, de Moraes RM, Bi T, Nayak RN, Sehgal YK, et al. The wide world of wide-area measurement. IEEE Power Energy Mag 2008;6(5):52–65.
[15] Skok S, Ivankovic I, Cerina Z. Applications based on PMU technology for improved power system utilization. In: IEEE power engineering society general meeting; 2007. p. 1–8.